Nature Communications

https://doi.org/10.1038/s41467-026-74757-8

Article in Press

Integrated proteomic and metabolomic analyses implicate redox-metabolic pathways in PTSD-associated multisystem disease and accelerated aging

Received: 12 January 2026

Accepted: 11 June 2026

Cite this article as: Kuan, P.-F., Mann, F.D., Yang, X. *et al.* Integrated proteomic and metabolomic analyses implicate redox-metabolic pathways in PTSD-associated multisystem disease and accelerated aging. *Nat Commun* (2026). https://doi.org/10.1038/s41467-026-74757-8

Pei-Fen Kuan, Frank D. Mann, Xiaohua Yang, Roman Kotov, Sean Clouston, Olga Ilkayeva, Michael Muehlbauer, Christopher B. Newgard & Benjamin J. Luft

Integrated proteomic and metabolomic analyses implicate redox-metabolic pathways in PTSD-associated multisystem disease and accelerated aging

Pei-Fen Kuan, PhD[1*], Frank D. Mann, PhD[2], Xiaohua Yang, MS[3], Roman Kotov, PhD[4], Sean Clouston, PhD[2], Olga Ilkayeva, PhD[5,6], Michael Muehlbauer, PhD[5], Christopher B. Newgard, PhD[5,6,7], and Benjamin J. Luft, MD[3*]

[1]Department of Applied Mathematics and Statistics, Stony Brook University, Stony Brook, NY, USA
[2]Department of Family and Preventive Medicine, Stony Brook University, Stony Brook, NY, USA
[3]Department of Medicine, Stony Brook University, Stony Brook, NY, USA
[4]Department of Psychiatry, Stony Brook University, Stony Brook, NY, USA
[5]Sarah W. Stedman Nutrition and Metabolism Center & Duke Molecular Physiology Institute, Duke University Medical Center, Durham, NC, USA
[6]Department of Medicine, Division of Endocrinology, Nutrition, and Metabolism, Duke University Medical Center, Durham, NC, USA
[7]Department of Pharmacology and Cancer Biology, Duke University Medical Center, Durham, NC, USA

*Corresponding Authors:
Benjamin J. Luft, MD
Edmund D. Pellegrino Professor of Medicine and Director, WTC Health Program
Department of Medicine
Stony Brook University
HSC T-16, Room 082A
Stony Brook, NY 11794-8166, USA
Email: Benjamin.Luft@stonybrookmedicine.edu

Pei-Fen Kuan, PhD
Professor
Department of Applied Mathematics and Statistics
Stony Brook University
Math Tower, Room 1-113
Stony Brook, NY 11794, USA
Email: PeiFen.Kuan@stonybrook.edu

Abstract (149 words, max 150 words)
Posttraumatic stress disorder (PTSD) is associated with increased risk of chronic disease and premature aging, yet underlying molecular mechanisms remain unclear. We performed plasma proteomics (SomaScan; 9,404 proteins) and targeted metabolomics (145 metabolites) in 393 World Trade Center responders (232 with PTSD, 161 trauma-exposed controls). A total of 114 proteins and seven metabolites were differentially expressed in PTSD. Top proteins included NCAN, BCAN, NCAM1, and GDF15. Top metabolites included serotonin, lactate, glutamic acid, and cystathionine. Integrative analyses showed coordinated proteomic-metabolomic alterations, with widespread correlations linking metabolites involved in redox and amino acid metabolism to synaptic and oxidative stress-related proteins. Gene ontology enrichment identified neuronal plasticity, immune activation, extracellular matrix remodeling, and oxidative stress. Proteomic organ aging analyses revealed accelerated aging in the pancreas, lung, and at the organismal level in PTSD. These results reveal a redox-metabolic mechanism through which PTSD may drive multisystem aging and elevate disease risk.

Introduction

Post-traumatic stress disorder (PTSD) is a chronic and often debilitating psychiatric condition that can arise after exposure to traumatic events. About 6.1% of U.S. adults are estimated to experience PTSD at some point in their lives [1], highlighting its significance as a public health concern. PTSD affects more than mental health: individuals with the disorder also face higher risks of cardiovascular disease, metabolic problems, neurodegeneration, and premature death [2-6]. These observations suggest that trauma leaves lasting marks on the body, though we still do not fully understand the molecular processes that link psychological stress to long-term physical illness. Current treatments, including psychotherapy and medications, are only partially effective, as seen in populations like World Trade Center (WTC) responders, where high rates of PTSD persist nearly two decades after 9/11 [7,8]. Thus, it is critical to delineate the molecular processes underlying PTSD to develop therapies that can prevent physical morbidity in people with PTSD.

For many years, biological studies of PTSD have focused on stress-responsive systems, especially hypothalamic-pituitary-adrenal (HPA) axis signaling and immune activity [9,10]. While these pathways explain immediate stress reactions, they do not capture the long-lasting, multisystem effects or aging-related consequences of PTSD. In animal studies, chronic stress is shown to affect processes shared across the brain, blood vessels, immune system, and other tissues including redox balance, mitochondrial function, and metabolism [11-13]. Disruptions in these processes appear to contribute to aging-related disease and may link trauma exposure to downstream tissue dysfunction [14]. Yet few human studies have examined whether stress produces coordinated molecular changes across multiple organ systems in PTSD.

High-dimensional molecular profiling offers a promising way to fill these gaps. Plasma proteomics allows for the direct measurement of proteins that control nearly all physiological processes, from intracellular to intercellular signaling [15]. Metabolomic profiling, which examines small molecules reflecting upstream gene and protein activity, provides a complementary view of biochemical states across the body [16]. By integrating proteomic and metabolomic data, we can uncover coordinated molecular networks that might be missed when each type of data is analyzed separately. This approach gives a more comprehensive, systems-level understanding of the biological changes associated with trauma [17-21].

Reproducibility in PTSD omics research has improved with larger datasets, but variability in sample types, processing methods, and assay platforms continues to present challenges [22,23]. Most PTSD proteomic studies, including those from our group, have used the Olink platform [17-19]. In our earlier study [17], we examined 276 plasma proteins across three Olink targeted panels (Neurology, Neuro Exploratory, and Cardiovascular II) and identified six proteins, including NCAN and BCAN, associated with PTSD and mild cognitive impairment. A follow-up study in a larger cohort of 936 responders to World Trade Center (WTC) disaster, using the Olink Neurology panel confirmed several of these findings, highlighting neuronal and vascular pathways in PTSD [18]. Complementing these proteomic findings, our previous metabolomics study identified metabolites involved in fatty acid mobilization and oxidation, sphingolipid signaling, and amino acid–based neuroimmune pathways relevant to innate immunity, inflammation, and neuronal excitability [20].

Only one previous study used the SomaScan 1.3K assay, which profiled 1,305 proteins in 340 veterans and 180 active-duty soldiers [24]. Olink panels generally cover fewer proteins, focusing on specific pathways or diseases, except for Olink Explore HT, which measures roughly 5,400 proteins. In contrast, SomaScan allows broader coverage: the v4 and 11K v5 assays quantify over 5,000 and 10,000 proteins, respectively. These assays also offer the unique ability to estimate organ-specific proteomic aging, including the heart, kidney, liver, and lung [25]. In studies of aging and disease, these organ-level aging estimates correlate with risks for cardiovascular, renal, and other chronic conditions, reflecting cumulative stress and systemic decline [25,26]. To date, organ-specific proteomic aging has not been studied in PTSD, despite evidence linking PTSD to cardiometabolic disease, kidney dysfunction, and accelerated systemic aging [2-6].

In this work, we expand previous proteomic studies of PTSD by using the SomaScan 11K v5 platform, which quantifies over 10,000 protein analytes, providing unparalleled insight into a broad span of proteomic markers across multiple biological systems. This was complemented by targeted metabolomic profiling of 145 metabolites across diverse biochemical classes. WTC responders provide a uniquely informative cohort, having experienced a discrete episode of intense trauma and been followed longitudinally with detailed clinical phenotyping [27]. PTSD is highly prevalent in this population and strongly associated with chronic disease burden [28], allowing examination of molecular correlates of trauma-related disease risk. In turn, integrating proteomic networks, metabolic signatures, and organ-specific aging estimates offers a unique opportunity to uncover multisystem molecular mechanisms connecting trauma to long-term organ dysfunction, thereby investigating both psychiatric and physical health vulnerabilities in the context of chronic PTSD.

Results

Characteristics of study groups

The analytic cohort consisted of 393 participants, including 232 with PTSD and 161 trauma-exposed controls. Participants with PTSD were, on average, three years older and had higher BMI, and greater WTC exposure severity compared to trauma-exposed controls ($p < 0.01$). Depressive symptom severity, measured by the PHQ-9, was also substantially higher among participants with PTSD ($p < 0.001$). Nonsteroidal anti-inflammatory drug (NSAID) use was modestly higher in the PTSD group ($p = 0.046$), while selective serotonin reuptake inhibitor (SSRI) use and medical comorbidities were substantially higher ($p < 0.001$). There were no significant differences between the PTSD and control groups with respect to gender, race, smoking status, or statin use (Table 1). To further contextualize the analytic sample relative to the broader WTC cohort, longitudinal PTSD symptom trajectory analyses showed that the subsample was enriched for individuals with higher baseline symptom burden and less favorable symptom trajectories over time, consistent with the targeted case-control sampling design (Supplementary Figure 8).

PTSD is associated with coordinated proteomic and metabolomic alterations

To characterize molecular alterations associated with PTSD, we performed differential analyses of plasma proteomics and targeted metabolomics. Figure 1A and B display the volcano plots of the proteomics and metabolomics data, respectively. For the proteomics data, there were approximately equal numbers of upregulated and downregulated proteins, whereas more metabolites were upregulated in PTSD. A total of 121 aptamer-based protein analytes,

corresponding to 114 unique proteins, were differentially expressed between PTSD and controls at FDR < 0.05 from our primary discovery models. At the aptamer level, 73 analytes were upregulated and 48 were downregulated; when collapsed to unique proteins, 68 were upregulated and 46 were downregulated. In contrast, 7 metabolites were differentially expressed at FDR < 0.05 (6 upregulated, 1 downregulated). Heatmaps of the significant proteins and metabolites are presented in Figures 1C and 1D.

The top ten protein analytes ranked by statistical significance were NCAM-120, NCAM1, GNPTG, NCAN, NPTXR, DNAJ89, MSTN, ANGPT2, GDF11 and GDF15, with GNPTG, DNAJ89, ANGPT2 and GDF15 showing upregulation in PTSD. The protein with the largest AUC was GDF15, with a value of 0.709, and was ranked tenth among differentially expressed protein analytes. The seven differentially expressed metabolites were lactate, serotonin, hydroxylysine, glutamic acid, cystathionine, proline, and sphingomyelin SM(d44:2). All except serotonin were upregulated in PTSD, highlighting alterations in energy and amino acid metabolism in affected individuals. Of note, glutamic acid and cystathionine, two metabolites linked to the system x_c^- transporter, were significantly upregulated in PTSD, while related metabolites in the same pathway (cysteine and cystine) showed similar upward trends ($p = 0.06$, FDR = 0.277 for cysteine and $p = 0.02$, FDR = 0.168 for cystine). The top metabolite, lactate is derived by glycolytic metabolism of glucose, which was also nominally upregulated in PTSD ($p = 0.005$, FDR = 0.07). Similarly, three metabolites produced by activation of lipolysis, namely glycerol ($p = 0.03$, FDR = 0.199), total ketones ($p = 0.01$, FDR = 0.154), and NEFA ($p = 0.02$, FDR = 0.168) were also nominally upregulated in PTSD. Together, these signatures of increased glycolytic metabolism of glucose and mobilization and oxidation of lipid stores, may suggest an increased catabolic state in individuals with PTSD.

Sensitivity analyses confirmed the robustness of these findings (Supplementary Data 1). When additionally adjusted for BMI, smoking status, and WTC exposure, effect size estimates across all 9,404 protein analytes were highly concordant with the primary model (Spearman $r_s = 0.93$), with complete directional agreement among the 121 protein analytes identified in the primary analysis. Although the number of FDR-significant analytes decreased under the more conservative model, 115 of the 121 protein analytes retained nominal significance ($p < 0.05$), indicating that the observed signal was largely preserved.

To further address potential confounding by smoking or extreme WTC exposure, analyses were repeated in participants who were never or former smokers and had low or intermediate exposure ($n = 263$). Effect size estimates remained highly concordant with those from the full cohort (Spearman $r_s = 0.883$), with 100% directional agreement among the 121 protein analytes (Supplementary Data 1).

Additional sensitivity analyses, including nonlinear adjustment for age and BMI and models adjusting for NSAID, SSRI, and statin use, as well as medical comorbidities, yielded highly consistent results (Spearman $r_s > 0.92$) with complete directional agreement among the 121 proteins (Supplementary Data 1). Restricting analyses to participants with minimal-to-mild depressive symptoms (PHQ < 10; $n = 233$) also produced highly concordant effect estimates (Spearman $r_s = 0.74$), with 100% directional agreement among the 121 protein analytes. Detailed results of these analyses are provided in Supplementary Note 1 and Supplementary Data 1.

Parallel sensitivity analyses for the metabolomics data yielded consistent results. Among the 7 metabolites identified in the primary analysis, most remained nominally significant after additional covariate adjustment and in restricted analyses, with complete directional concordance (Supplementary Data 1).

In our secondary analysis of tryptophan (Trp)-related and branched chain amino acid (BCAA)-related metabolites, including the branched chain ketoacids (BCKA) and branched chain hydroxyacid (BCHA) metabolites, duplicated measurements of tryptophan, kynurenine, and serotonin across the primary and secondary metabolomics datasets showed moderate-to-high reproducibility (Supplementary Figure 3). Five metabolites were identified at nominal significance ($p < 0.05$) (Supplementary Table 1): three Trp-related metabolites including indole-3-propionic acid (down), indole-3-lactic acid (up), and kynurenic acid (down), and two BCHA metabolites including 2-hydroxy-3-methylvaleric acid (HMVA) (up) and 2-hydroxyisovaleric acid (HIVA) (up). Among these, indole-3-propionic acid, HMVA and indole-3-lactic acid also remained significant at FDR < 0.05 when the FDR correction was restricted to the secondary metabolomics dataset. Additional analyses involving this dataset are provided in Supplementary Note 3 and Supplementary Figures 4-7.

Proteomic and metabolomic signatures show strong concordance with prior PTSD studies

Our findings showed strong concordance with prior proteomic and metabolomic investigations. In our earlier targeted proteomic analysis using Olink panels covering 276 proteins [17], eleven of the 121 differentially expressed protein analytes identified in the present work were measured, yet all (NCAN, MSTN, KYNU, BCAN, RGMA, THBS2, IL1RN, FGF21, ASGR1, and KITLG) but one (PIGR) demonstrated consistent effect directions, with NCAN and BCAN reaching statistical significance in both datasets (Table 2). When comparing proteins previously associated with comorbid PTSD and mild cognitive impairment in our earlier study [17], the ten corresponding aptamers in the present dataset also showed a high degree of directional agreement: eight demonstrated effects in the same direction (Supplementary Data 2).

Our second prior study [18], which analyzed 92 neurologically relevant proteins in a larger cohort of 936 WTC responders, identified ten proteins associated with PTSD diagnosis or symptom severity (PCL total scores). These proteins corresponded to sixteen aptamers in the current analysis, and most showed consistent effect directions, including replicated associations for NCAN and BCAN, i.e., two proteins repeatedly emerging across studies (Supplementary Data 2). Results were comparable in subset analyses by excluding all participants who overlapped with either prior study ($n = 91$ removed) (Supplementary Data 2).

We observed a strong convergence when comparing our findings with the recent PSYCHENCODE2-UKBB PTSD proteomic study [19], which assessed 2,941 plasma analytes using Olink Explore 3072 and identified 299 PTSD-associated proteins. Of the 339 corresponding aptamers (some proteins have multiple aptamers) in our dataset, 244 (72%) showed consistent effect directions and 98 achieved nominal significance ($p < 0.05$), demonstrating broad reproducibility across platforms (Supplementary Data 2). Notably, 32 of the 121 differentially expressed protein analytes in our study overlapped directly with the PSYCHENCODE2-UKBB

set, including NCAM1, BCAN, and GDF15 (Table 2). Among these overlapping analytes, 31 of 32 showed consistent effect directions.

Finally, six of the 121 differentially expressed protein analytes (NCAM-120, NCAM1, EGFR, CNTN1, SLITRK5, and UNC5D) overlapped with the 36 PTSD-relevant proteins identified by Muhie et al. [24] through network-based analyses incorporating genetic associations (Table 2), providing further evidence that the molecular signals observed here converge with those reported in a different population.

For metabolomics, our findings also aligned with our prior Metabolon-based study [20], which identified hexosylceramide HCER(26:1) as upregulated in PTSD. In the present study, this metabolite also showed higher levels in PTSD, though it was not statistically significant (nominal $p = 0.221$). Moreover, all seven significant metabolites identified in the present study showed consistent effect directions compared to our previous results [20]. Serotonin, in particular, was nominally significant ($p < 0.05$) in our earlier study.

PTSD-associated molecular alterations implicate neuronal, immune, and extracellular matrix pathways

Gene Ontology (GO) enrichment analysis of proteomics data identified 25 significantly enriched categories at FDR < 0.1 (Table 3). Twelve were directly related to neuronal processes, including neuron projection regeneration, glial cell differentiation, gliogenesis, axon regeneration, response to axon injury, regulation of nervous system development, regulation of axon regeneration, regulation of neuron projection regeneration, negative regulation of neuron projection regeneration, axon development, regulation of neurogenesis, and glial cell development. Additional categories included immune function, oxidative stress and inflammatory pathways, extracellular matrix (ECM) structure, developmental and growth regulation, and nutrient metabolism. No KEGG pathways reached statistical significance at FDR < 0.1.

Results from Independent Component Analysis (ICA) identified top modules associated with PTSD that were enriched in pathways related to neuronal development, axon guidance, and synaptic organization; extracellular matrix structure and cell adhesion; growth factor and receptor-mediated signaling; immune and inflammatory processes; and developmental and morphogenetic programs related to tissue remodeling (Supplementary Note 2 and Supplementary Data 5).

Integrated proteomic-metabolomic analyses reveal cystine-glutamate and redox dysregulation in PTSD.

Integrative analysis of proteomic and metabolomic data revealed coordinated molecular alterations in PTSD. Across the seven significant metabolites, 120 protein analytes were significantly correlated with at least one of the metabolites (Figure 2A). The number of correlated protein analytes varied by metabolite: 104 with lactate, 96 with cystathionine, 108 with glutamic acid, 108 with hydroxylysine, 71 with proline, and 36 with serotonin. No proteins were significantly correlated with sphingomyelin SM(d44:2) at the FDR < 0.05 threshold, indicating that it did not show strong coordinated associations in this dataset. Among these 120 protein analytes, eighteen protein analytes (NCAM-120, NCAM1, GDF15, HTRA1, RP9, MORC3, ACSM4, THBS2, PXDN, CNTN1, GBE1, MPST, GOLM1, NBPF1, NCF2, NCKAP5, TNFRSF10D, and FABP4) were correlated with six of the seven metabolites, suggesting they may act as hub proteins driving

multi-omic dysregulation in PTSD. Notably, GDF15, a key mediator of cachexia and catabolic metabolism was broadly correlated across metabolites, consistent with a central role in systemic metabolic and stress-response dysregulation in PTSD.

At FDR < 0.05, no protein-metabolite interaction terms remained statistically significant by PTSD status. At a nominal threshold of $p < 0.01$, six protein-metabolite pairs showed evidence of interaction, including cystathionine versus NCAN, cystathionine versus NOX4, cystathionine versus ENPP5, cystathionine versus CACNA2D3, hydroxylysine versus MXRA8, and serotonin versus MORC3 (Figure 2). We therefore performed exploratory stratified analyses by PTSD status for these six pairs. In five pairs (cystathionine versus NCAN, cystathionine versus NOX4, cystathionine versus ENPP5, cystathionine versus CACNA2D3, and hydroxylysine versus MXRA8), the metabolite-protein association was stronger and statistically significant among participants with PTSD, while associations were weak or non-significant in trauma-exposed controls. In contrast, the serotonin versus MORC3 association appeared stronger in controls than in participants with PTSD. Stratified results are provided in Supplementary Data 3. Although these findings suggest potential PTSD-related differences in selected metabolite-protein relationships, interaction terms did not survive multiple testing correction and should therefore be interpreted as exploratory.

Supplementary Figure 2 presents pairwise (protein-metabolite) plots of metabolites associated with the system x_c^- transporter (glutamic acid, cystathionine, cysteine, cystine) and NOX4, showing generally positive correlations. Beyond the cystathionine-NOX4 pair, the cysteine-cystine and cystathionine-glutamic acid pairs also exhibited stronger correlations in the PTSD group compared with controls, highlighting altered regulation of system x_c^--related metabolic pathways in PTSD.

PTSD is associated with accelerated proteomic aging across multiple organ systems

We next used our proteomics data set to examine whether PTSD was associated with accelerated biological aging across multiple organ systems. The Spearman rank correlations between predicted age measures and chronological age ranged from 0.222 to 0.843 (Table 4), where the global aging measures showed strong associations with chronological age (Conventional: Spearman $r_s = 0.843$; Organismal: Spearman $r_s = 0.826$; CognitionOrganismal: Spearman $r_s = 0.721$). Five of the 25 age measures were significantly associated with PTSD at FDR < 0.05: Pancreas, CognitionLung, Organismal, CognitionOrganismal, and Conventional (Figure 3). In all cases, PTSD participants exhibited accelerated predicted biological aging compared to trauma-exposed controls. These findings suggest that molecular signatures of PTSD extend beyond brain-related processes to encompass systemic alterations in metabolic and organ-specific aging.

Enrichment analyses of the full ranked proteomic results from the PTSD differential expression analysis revealed significant enrichment for brain-specific proteins. Among the 121 differentially expressed protein analytes, seven proteins (BCAN, OMG, SEZ6L, CNTN1, NPTXR, NCAN, and IGLON5) overlapped with brain-specific proteins identified by [12] (Supplementary Data 4).

Discussion

In this study, we used large-scale plasma proteomics and targeted metabolomics to study the molecular changes associated with post-traumatic stress disorder (PTSD) in World Trade Center responders, nearly 18 years after the 9/11 attacks. Using primary discovery models adjusted for age, gender, and race, together with robust inference with heteroskedasticity-consistent (HC3) standard errors, we identified 121 aptamer-based protein analytes (114 unique proteins) and 7 metabolites that were differentially expressed in individuals with PTSD. These molecular signatures converge on pathways related to neuronal structure, immune activation, extracellular matrix remodeling, metabolic regulation, and redox balance. Beyond replicating previously reported proteomic and metabolomic changes, our findings provide important insights into system x_c⁻ metabolite dysregulation and reveal coordinated multi-omic patterns linking sulfur amino acid metabolism, oxidative stress, and tissue remodeling. In addition, we observed evidence of accelerated biological aging across multiple organ-enriched plasma proteomic signatures. Together, these findings indicate that PTSD is accompanied by coordinated, multisystem molecular dysregulation that extends well beyond the central nervous system and provides insight into the long-term biological embedding of traumatic stress.

In our proteomic analyses, we observed a mix of proteins that were upregulated or downregulated in PTSD. Among these were NCAN, BCAN, NCAM1, and GDF15, i.e., proteins that have been previously linked to psychiatric disorders, neurodegeneration, and stress-related biology [17-19]. Interestingly, GDF15 stood out as having the strongest discriminative ability. This protein has been associated with mitochondrial stress, systemic inflammation, cachexia, and cellular senescence [29,30], suggesting that it could be a meaningful marker of PTSD-related biological changes. Furthermore, our result is consistent with earlier Olink-based studies from our group [17,18] and largely overlaps with the large-scale PSYCHENCODE2-UKBB list of PTSD-associated proteins [19]. Moreover, some of these proteins also appeared in co-expression network analyses that mapped to genetic variants linked to PCL scores in military personnel [24]. Taken together, these results point toward a set of core molecular signals that may contribute to PTSD risk across different populations.

Our metabolomic analysis highlighted alterations in energy metabolism and excitatory neurotransmission. Specifically, elevated lactate and glutamic acid indicate shifts in glycolytic flux and excitatory signaling [31], while elevation of cystathionine in concert with glutamic acid suggests dysregulation of the system x_c⁻ antiporter, which regulates glutamate-cystine exchange and oxidative stress regulation [32]. This finding is supported by similar upward trends in two other system x_c- metabolites, cysteine and cystine, with cystine reaching nominal significance and cysteine showing a comparable trend. Upregulation of lactate, glycerol, ketones, and NEFA indicates an increased catabolic state and altered systemic energy utilization in PTSD, consistent with prior findings of disrupted energy metabolism in PTSD [20,33]. These findings may relate to the increase in GDF15, a circulating peptide that acts centrally to cause reductions in food intake and peripherally to enhance lipolysis and fatty acid oxidation [34]. Serotonin was reduced among PTSD cases in the present study, consistent with decades of evidence for serotonergic dysfunction in trauma-related disorders, although the direction of regulation has been mixed across studies [35,36], partly due to differences in biospecimen types. The downregulation pattern observed here may contribute to specific symptoms of PTSD, including hyperarousal, irritability, and sleep disturbance [35], and is also consistent with the clinical efficacy of selective serotonin reuptake

inhibitors (SSRIs) for treatment of PTSD [37]. We note that global upregulation of glutamatergic and oxidative stress signaling supports excitotoxicity and redox disruption models of chronic PTSD [38,39], suggesting that serotonergic, metabolic, and immune signaling dysregulation may collectively drive both psychiatric illness and systemic biological alterations. Secondary analyses of tryptophan (Trp)-, BCAA-related metabolites suggested PTSD-related dysregulation of BCAA, tryptophan, and kynurenine pathways, further reinforcing alterations in redox balance, mitochondrial function, and stress-related pathways.

Our gene ontology analysis revealed processes involved in neuronal development and repair, including axon regeneration, synapse organization, and glial differentiation. These results are in line with evidence that maladaptive plasticity and abnormal remodeling of neural circuits are important features of PTSD [40]. We also observed enrichment of immune, inflammatory, and extracellular matrix pathways, reinforcing the systemic nature of PTSD biology and the interplay between neuroinflammation, tissue remodeling, and peripheral immune dysregulation [10]. Notably, despite the chronicity of PTSD in our participants, our findings show enrichment of pathways related to neuronal regeneration, suggesting the presence of molecular repair processes long after the traumatic event, and in some cases decades later. Findings from Independent Component Analysis (ICA) reinforce this view, indicating that PTSD involves coordinated disruptions across immune, structural, and neuronal systems, which aligns with the patterns seen in our differential expression and pathway analyses.

In integrative proteome-metabolome analyses, we observed broad coordinated associations between the significant metabolites and many protein analytes, consistent with multi-omic coupling of metabolic and proteomic systems. However, protein-metabolite interaction terms did not remain statistically significant after multiple testing correction. At a nominal threshold, a small number of pairs showed suggestive evidence of differential metabolite-protein slopes by PTSD status, including cystathionine with synaptic, ECM and oxidative stress-related proteins (e.g., NCAN and NOX4), as well as hydroxylysine with MXRA8. Exploratory stratified analyses suggested that several of these metabolite-protein associations were stronger among participants with PTSD. Cystathionine is an important metabolite in transsulfuration that links methionine metabolism with glutathione synthesis and cellular redox stabilization [32]. The stronger association with NCAN (which regulates the composition of the extracellular matrix and synaptic stability [41]) suggest that sulfur amino acid metabolism may regulate neuronal structural remodeling associated with PTSD. In addition, hydroxylysine, a collagen-derived amino acid associated with extracellular matrix turnover [42], showed a nominal interaction with MXRA8, a matrix-remodeling-associated protein [43], further supporting a potential link between metabolite signals of ECM remodeling and proteomic markers of tissue structural regulation. This observation is consistent with our enrichment analyses, which highlighted extracellular matrix organization and tissue remodeling as prominent biological themes in the PTSD-associated proteomic signatures. We also observed a robust correlation with NOX4, which generates reactive oxygen species and mediates signaling related to oxidative stress [44], thus offering a potential mechanistic link between metabolic dysregulation and oxidative/inflammatory pathways. Furthermore, the elevation of GDF15 observed in PTSD is consistent with the upregulation of the stress response downstream of redox and mitochondrial dysfunction, offering a potential systemic correlate of the metabolic and oxidative stress signatures that we identified through our proteome-metabolome analysis. Because these interaction effects did not survive FDR correction, they should be interpreted as exploratory

and hypothesis-generating. Nonetheless, they provide biologically coherent candidates linking sulfur amino acid metabolism to oxidative stress and neuronal or ECM remodeling in chronic PTSD.

Supplementary Figure 2 further supports these observations, showing that metabolites associated with the system x_c⁻ transporter (glutamic acid, cystathionine, cysteine, cystine) exhibit generally positive correlations with each other, with stronger pairwise relationships among PTSD cases compared to controls. Notably, cystathionine-glutamic acid and cysteine-cystine correlations were heightened in PTSD, reinforcing dysregulation of glutamate-cystine exchange and redox balance [32]. Given the role of system x_c⁻ in regulation of cellular redox status via synthesis of glutathione [32], these findings could indicate alterations in responses to oxidative stress in PTSD. Altogether, these findings suggest a coordinated shift in metabolic protein networks that couple sulfur amino acids, excitatory neurotransmission, and oxidative and inflammatory states with protein markers for synaptic and extracellular matrix remodeling.

An important finding of our study is that PTSD is associated with accelerated proteomic aging across multiple organ-enriched plasma signatures, including the pancreas and lung, as well as at the organismal level. In particular, accelerated pancreatic aging suggests that long-term trauma exposure may be linked to earlier declines in pancreatic function, although our analysis at this stage does not discriminate the endocrine from the exocrine pancreas. The combination of dysregulation of glutamate-cystine exchange and redox balance, and possible alterations in pancreatic hormone secretion could contribute to the observed increase in the risk of metabolic diseases such as type 2 diabetes in subjects with PTSD [5]. We also found that both conventional and cognition-informed proteomic aging models were accelerated in PTSD, reinforcing PTSD as a systemic condition that accelerates aging. These findings extend prior work linking PTSD to telomere shortening [45], DNA methylation and transcriptomic age acceleration [3,46], and heightened risk of age-related disease [2,4-6]. Importantly, complementary enrichment analyses revealed that PTSD-associated proteomic alterations are not randomly distributed but are preferentially enriched among brain-specific proteins. The overlap of multiple differentially expressed proteins with brain-specific markers, of which many are involved in synaptic structure and neuronal connectivity, provides convergent evidence that central nervous system-relevant molecular perturbations are detectable in plasma long after trauma exposure. Together, the organ-level insights provided by proteomic aging models [25] reveal that PTSD may affect different physiological systems in distinct ways, highlighting the potential of organ-specific biomarkers to predict long-term health outcomes in this high-risk population. At the same time, we emphasize that these plasma-based “organ age” measures should not be interpreted as reflecting proteins exclusively expressed in a single organ or as direct measurements of tissue-specific aging. Rather, they represent plasma-derived aging signatures constructed from protein sets enriched for organ-predominant expression (as defined using transcriptomic reference atlases) and validated in prior work against organ-relevant outcomes [25]. Thus, the observed associations support the interpretation that PTSD relates to systemic aging biology captured by organ-enriched plasma proteomic patterns, while acknowledging the inherent limitation that plasma signals cannot uniquely localize biological processes to specific tissues.

Our findings were robust across multiple sensitivity analyses in both proteomic and metabolomic data. Effect estimates remained consistent after adjusting for BMI, smoking status, and WTC

exposure, as well as in analyses restricted to never or former smokers with lower exposure. Additional adjustment for medical comorbidities and medication use had minimal impact on the results. Restricting analyses to participants with minimal-to-mild depressive symptoms yielded similar patterns, indicating that the observed molecular signatures are not driven solely by depressive symptoms. Overall, these findings suggest that the identified signatures reflect the broader biology of chronic PTSD in a real-world, comorbid population rather than "pure" PTSD in isolation.

One of the key strengths of this study is the integration of large-scale proteomic and metabolomic data within a well-characterized cohort, along with replication against prior datasets and the innovative use of validated organ-enriched aging signatures. Together, these approaches provide a broad and detailed view of the molecular changes linked to PTSD. Nonetheless, our findings must be considered in the context of several limitations. While the WTC cohort offers a unique chance to study trauma-related biology in people with a shared exposure history, the analytic sample represents an enriched case-control design drawn from a larger parent cohort and may not be representative of cohort-wide distributions; replication in independent PTSD populations will be necessary to confirm that our findings generalize more broadly. Another limitation is that plasma-based proteomics and metabolomics may not fully capture events in the brain or other organs; complementary studies using cerebrospinal fluid, neuroimaging, or postmortem brain and other tissue sampling could provide deeper insight. Despite extensive sensitivity analyses, residual confounding by unmeasured clinical, environmental, and treatment-related factors could still have influenced our results. Finally, because this analysis was cross-sectional, we cannot determine causality or directionality of the associations observed. Given that biospecimens were collected many years after the initial trauma exposure, the molecular signatures identified here likely reflect long-term biological embedding of chronic PTSD rather than acute post-trauma responses. This interpretation is further supported by longitudinal PTSD symptom trajectory analyses [47], which indicate that the analytic subsample was enriched for individuals with persistently elevated symptom burden and less favorable symptom trajectories over time, consistent with chronic rather than transient PTSD. Longitudinal research will be crucial to test whether these biomarkers can predict disease progression, treatment response, or longer-term health outcomes.

In conclusion, we present one of the most comprehensive proteomic and metabolomic profiles of PTSD to date. Our analyses uncover reproducible protein and metabolite signatures, crosstalk between molecular pathways, and point to accelerated biological aging across multiple organs. Together, these findings link PTSD to neuronal, immune, metabolic, and aging-related processes, emphasizing its systemic nature and informing future biomarker research.

Methods

Participants and PTSD assessment

Participants were recruited from the Stony Brook World Trade Center (WTC) Health Program [27]. The study was approved by the Stony Brook University Institutional Review Board, and all participants provided written informed consent. Blood samples were collected in 2019, nearly 18 years after the 9/11 attacks. Inclusion criteria required sufficient English language proficiency to complete the study protocol. Both male and female participants were eligible. Gender information was obtained through participant self-report and was included as a covariate in all primary

statistical analyses. Participants did not receive financial compensation for participation in this study. Responders with a history of head injuries, brain tumors, or cancers were ineligible for the study.

Probable PTSD was assessed using the 17-item Posttraumatic Stress Disorder Checklist for a specific stressor (PCL-S) [48], a validated self-report measure based on DSM-IV criteria. Participants rated items on a 5-point Likert scale (1 = "not at all" to 5 = "extremely"), with excellent internal consistency (Cronbach's $\alpha = 0.96$). A PCL total score > 43 was used to indicate probable PTSD. The trauma-exposed control group was defined as asymptomatic (PCL total score < 23) and underwent an additional medical record review to exclude individuals with a clinical history of other psychiatric disorders, including major depressive disorder. Participants meeting criteria for probable PTSD were not excluded on the basis of psychiatric comorbidities. The analytic sample was assembled using an enriched case-control design from the larger WTC responder cohort, resulting in overrepresentation of individuals at the extremes of PTSD symptom burden. Accordingly, the case-control composition does not reflect the prevalence of PTSD in the broader WTC cohort.

Depressive symptom severity was assessed using the Patient Health Questionnaire-9 (PHQ-9) [49], a validated 9-item self-report measure of depressive symptoms over the past two weeks. Items are rated on a 4-point Likert scale (0 = "not at all" to 3 = "nearly every day"), yielding a total score ranging from 0 to 27, with higher scores indicating greater depressive symptom burden.

The analytic cohort included 393 participants (232 PTSD, 161 trauma-exposed controls), with a mean age of 55.5 years (SD = 7.7), 87% White, and 41% current or former smokers. Additional covariates included body mass index (BMI) and exposure [50]. Exposure was defined using a composite measure incorporating duration of work at the WTC site, exposure to the dust cloud from the collapse of the buildings, and work on the debris pile. Participants were categorized into four ordered exposure groups (low, intermediate, high, and very high), reflecting increasing exposure intensity [50].

Physician-diagnosed medical conditions were abstracted from electronic medical records within the WTC Health Program. A composite medical comorbidity variable was defined as the presence of chronic obstructive pulmonary disease, cardiac disease, diabetes mellitus, hypertension, or stroke (any vs none).

Current medication use at the time of blood draw was assessed using structured clinical intake forms, incorporating both program records and participant self-report. Nonsteroidal anti-inflammatory drug (NSAID) use included both prescription and over-the-counter medications. Selective serotonin reuptake inhibitor (SSRI) use and statin use were similarly defined using combined program and self-reported data. All medication variables were coded as binary indicators (yes/no) reflecting use at the study visit.

To contextualize the analytic sample relative to the broader WTC cohort, longitudinal PTSD symptom trajectories derived from repeated PCL assessments were compared between the analytic subsample and the full cohort (Supplementary Figure 8).

Blood sampling

Participants were instructed to fast for at least 8 hours and to refrain from NSAID use, aspirin, and vigorous exercise on the morning of blood collection. Blood draws were conducted under standardized clinical procedures during routine WTC Health Program visits. Whole blood was collected into K2-EDTA tubes (BD Vacutainer, Franklin Lakes, NJ), gently inverted 8-10 times, and centrifuged at 2,000 × g for 15 minutes at 4 °C. Plasma was aliquoted into polyethylene tubes and stored at −80 °C until analysis.

Proteomics profiling

Plasma proteins were quantified using the SomaScan 11K v5 assay, a high-throughput multiplex platform based on modified single-stranded DNA aptamers, which provide high specificity and sensitivity. The assay measures more than 11,000 aptamer-based protein analytes, comprising over 10,000 aptamers representing more than 9,600 unique human proteins; some proteins are represented by multiple aptamers. These target analytes span a broad range of biological pathways, including neurology, cardiology, inflammation, and oncology. Additional details are available elsewhere (https://somalogic.com/).

Proteomics data preprocessing

Protein abundances were quantified as relative fluorescence units (RFU). Normalization included the following steps: (i) hybridization normalization to reduce readout bias, (ii) intraplate median normalization to correct for within-plate variation, (iii) plate scaling for between-plate variation, (iv) calibration to minimize run-to-run variability, and (v) Adaptive Normalization by Maximum Likelihood (ANML) to adjust for inter-sample variability. Quality control (QC) was performed by comparing replicate signals against reference standards.

RFU values were log10-transformed and standardized. Samples failing Somalogic-provided row-level QC (RowCheck flag; $n = 2$) and non-human aptamers ($k = 295$) were removed. Analytes were further filtered based on assay QC performance (QC CV < 0.1 and ≤ 2 plates with calibration QC ratios outside 0.8-1.2). The final dataset included 391 participants (231 with PTSD, 160 controls) and 9,404 aptamer-based protein analytes targeting 8,514 unique human proteins.

To evaluate potential batch effects, we examined the distribution of PTSD cases and controls across assay plates and assessed sample clustering using principal component analysis (PCA) of normalized proteomic data. There was no significant association between plate and PTSD status (chi-square test $p = 0.28$), indicating comparable distribution of cases and controls across plates. Visualization of the first two principal components demonstrated no clustering by assay plate or PTSD status (Supplementary Figure 1).

We also examined inter-individual variability across all log10-transformed proteomic analytes prior to differential analyses. Variability was assessed using the standard deviation (SD) and median absolute deviation (MAD) of log10-transformed, unscaled data. The distribution of these measures across 9,404 aptamers indicated substantial variability, with no evidence of a substantial

subset of near-invariant features (SD: median = 0.114, IQR = 0.087-0.156; range = 0.009-1.085; MAD: median = 0.067, IQR = 0.046-0.106; range = 0.008-0.730). Accordingly, no additional variability-based filtering was applied.

Metabolomics profiling

Metabolomic profiling was performed using five custom panels targeting 145 metabolites, including 5 conventional metabolites, 44 amino acids and biogenic amines, 21 ceramides, 30 sphingomyelins, and 45 acylcarnitines. These panels were chosen to capture direct and indirect pathways including fatty acid mobilization and oxidation, sphingolipid signaling, and amino acid-based neuroimmune pathways relevant to innate immunity, inflammation, and neuronal excitability identified from our previous work [20].

Acylcarnitines were quantified by flow injection tandem mass spectrometry (MS/MS) as previously described [51], using a Waters Xevo TQD mass spectrometer coupled with an Acquity™ UPLC system. Amino acids and biogenic amines were measured by LC-MS/MS following an adapted method from [52]. Briefly, 10 µL of plasma was spiked with stable isotope-labeled standards, deproteinized with methanol, and derivatized with AccQTag reagent at 55 °C. Separation was performed on a Waters Acquity UPLC HSS T3 column using a formic acid-acetonitrile gradient, and analytes detected in positive ion mode via multiple reaction monitoring (MRM) on a Xevo TQ-XS system. Ceramides and sphingomyelins were extracted as described previously [53] and analyzed by MS in positive ionization mode. Conventional metabolites, including glucose, lactate, glycerol, non-esterified fatty acids (NEFA), and total ketone bodies, were quantified using a Beckman-Coulter DxC 600 clinical analyzer, as previously described [54].

Metabolomics data were available for 356 participants (213 with PTSD, 143 controls). For acylcarnitines, limited plasma availability yielded data for 333 participants (196 with PTSD, 137 controls). All metabolite values were log10-transformed. Inter-individual variability was assessed using the standard deviation (SD) and median absolute deviation (MAD) of log10-transformed metabolite levels. The distributions indicated adequate dispersion across participants (SD: median = 0.155, IQR = 0.118-0.257; range = 0.066-2.569; MAD: median = 0.139, IQR = 0.108-0.181; range = 0.065-1.053), with no evidence of near-invariant metabolites.

Secondary metabolomics profiling included 10 additional tryptophan pathway metabolites, 3 branched-chain hydroxy acid (BCHA) metabolites, and 3 branched-chain keto acid (BCKA) metabolites in 276 participants (165 with PTSD, 111 controls). Tryptophan pathway metabolites were analyzed on a Waters Xevo TQ-XS triple quadrupole mass spectrometer (Milford, MA) coupled to a Waters Acquity UPLC system using a HSS T3 column (1.8 µm, 2.1 × 150 mm), as described previously [55]. BCHA metabolites were quantified by LC-MS/MS using a Waters Xevo TQ-XS system coupled to a Waters Acquity UPLC, as reported previously [56]. BCKA metabolites were analyzed by LC-MS/MS as previously described [57], using isotopically labeled internal standards KIC-d3, KIV-5C13 (Cambridge Isotope Laboratories), and KMV-d8 (Toronto Research Chemicals).

Differential proteomics and metabolomics analysis

For primary discovery models, separate linear regression analyses were performed for each aptamer-based protein analyte and metabolite, using log10-transformed that were subsequently standardized (z-scored) analyte levels as the dependent variable and PTSD status as the independent variable, adjusting for age, gender, and race. To account for potential heteroskedasticity and influential observations, regression models were re-estimated using heteroskedasticity-consistent (HC3) standard errors. Robust Wald tests were implemented using the sandwich (v3.1.1) and lmtest (v0.9.40) packages in R. A false discovery rate (FDR) < 0.05 was used to identify significant proteins and metabolites. The area under the receiver operating characteristic curve (AUC) was also computed to assess discriminative power of each analyte.

To evaluate potential confounding by environmental and lifestyle factors, primary models were additionally adjusted for BMI, smoking status, and WTC exposure. WTC exposure was modeled as an ordinal variable (low, intermediate, high, very high) to reflect increasing exposure intensity. Additional analyses were performed in a restricted subset of participants who were never or former smokers and had low or intermediate exposure levels. Sensitivity analyses further evaluated the robustness of findings to alternative model specifications. To assess potential nonlinear confounding, models incorporating quadratic terms (Age^2 and BMI^2) and natural spline functions (*df* = 3) for age and BMI were examined. Additional models adjusted for medical comorbidities and medication use (NSAIDs, SSRIs, and statins), including analyses excluding NSAID users. Given the high comorbidity between PTSD and depressive symptoms, analyses were also repeated after restricting participants to those with minimal-to-mild depressive symptoms (PHQ < 10). Parallel sensitivity analyses were performed for the metabolomics data.

Results were compared with findings from our prior proteomics studies [17,18], our metabolomics study [20], the PSYCHENCODE2 PTSD study utilizing UKBB plasma proteomics [19] and a study of military personnel [24]. Among the 391 participants with proteomics data in the current study, 88 overlapped with our first prior study [17] and 91 overlapped with our second prior study [18]. To evaluate the independence of the present findings, we conducted sensitivity analyses excluding all participants who overlapped with either prior study (*n* = 91 removed).

Differential metabolomics analyses were also performed on the secondary metabolomics dataset, which included tryptophan-, BCHA-, and BCKA-related metabolites. Due to the smaller sample size (*n* = 276), this dataset was not included in primary integrative analyses.

Pathway analysis

Pathway enrichment was performed on differentially expressed proteins using Gene Ontology (GO) terms [58] and KEGG canonical pathways [59].

Integrative proteomics-metabolomics analysis

We performed an integrative analysis by examining the correlations and potential synergy (i.e., interaction effects) between differentially expressed protein analytes and metabolites to further characterize coordinated molecular alterations. Specifically, Spearman rank correlation analyses and linear regression models were applied to test whether protein-metabolite relationships differed between individuals with PTSD and trauma-exposed controls. Potential moderation effects were evaluated using product interaction terms in the regression models (protein analyte × case status),

adjusting for age, gender, and race. For protein-metabolite pairs demonstrating evidence of interaction at a nominal threshold ($p < 0.01$), exploratory stratified analyses were conducted within PTSD and control groups separately to estimate group-specific slopes. As in the differential expression analyses, statistical inference was based on heteroskedasticity-consistent (HC3) standard errors and robust Wald tests. Statistically significant protein-metabolite interactions were defined at a metabolite-wise FDR < 0.05.

Independent component analysis (ICA) was performed to identify modules of co-expressed protein analytes and metabolites [60]. Each module was then refined by retaining proteins with significant contribution scores (FDR < 0.05). Associations between ICA modules and PTSD were examined using linear regression models adjusted for age, gender, and race, with statistical significance defined at FDR < 0.05. Pathway enrichment analysis was conducted for significant modules using Gene Ontology (GO) terms [58].

Organ aging

Organ-specific proteomic ages were generated using a validated plasma-based organ age calculator for 11 organs (adipose, artery, brain, heart, immune system, intestine, kidney, liver, lung, muscle, and pancreas) [25]. Two sets of models were used: (i) organ-specific models trained on corresponding proteins and (ii) "CognitionX" models trained on proteins identified by the FIBA algorithm applied to CDRGLOB (global clinical dementia rating), incorporating both chronological age and cognitive decline.

Additionally, three global measures were estimated: Conventional (all proteins), Organismal (organ non-specific proteins), and CognitionOrganismal (CDRGLOB-FIBA trained). Altogether, 25 age estimates were derived.

Spearman rank correlations were computed between each predicted organ age and chronological age to evaluate age-tracking performance.

For each estimate, an "age gap" was calculated as the difference between predicted and expected age relative to same-aged peers from the models' training cohort. Associations between age gaps and PTSD were tested using linear regression, adjusted for chronological age, gender, and race, with statistical significance defined at FDR < 0.05 based on heteroskedasticity-consistent (HC3) standard errors and robust Wald tests.

We also assessed overlap between our differentially expressed protein analytes and organ-specific protein sets used to train the organ aging models in [25], and performed enrichment analyses using the full ranked list of protein analytes ranked by the product of -log p-value and effect size direction for each organ, with statistical significance defined at FDR < 0.05.

Data availability

Summary statistics from association analyses of all analyzed proteins and metabolites have been deposited in the Open Science Framework (https://osf.io/z5hse). Individual-level clinical and omics data cannot be publicly shared in order to protect the privacy and confidentiality of World

Trade Center responders and due to ethical restrictions governing human subjects research. De-identified individual-level data may be made available to qualified researchers through the Stony Brook World Trade Center Health and Wellness Program by contacting Dr. Benjamin Luft (Benjamin.Luft@stonybrookmedicine.edu). Access is subject to Institutional Review Board approval, applicable data use agreements, and institutional policies governing human subjects research. Source data are provided with this paper.

Code availability

Analyses were conducted in R (v4.4.2). The analysis code has been deposited in the Open Science Framework (https://osf.io/z5hse).

References

1. Koenen, K.C., *et al.* Posttraumatic stress disorder in the World Mental Health Surveys. *Psychol Med* **47**, 2260-2274 (2017).
2. Koraishy, F.M., *et al.* The association of posttraumatic stress disorder with longitudinal change in glomerular filtration rate in world trade center responders. *Biopsychosocial Science and Medicine* **83**, 978-986 (2021).
3. Kuan, P.-F., *et al.* PTSD is associated with accelerated transcriptional aging in World Trade Center responders. *Translational psychiatry* **11**, 1-8 (2021).
4. Rosenbaum, S., *et al.* The prevalence and risk of metabolic syndrome and its components among people with posttraumatic stress disorder: a systematic review and meta-analysis. *Metabolism* **64**, 926-933 (2015).
5. Vancampfort, D., *et al.* Type 2 diabetes among people with posttraumatic stress disorder: systematic review and meta-analysis. *Psychosomatic medicine* **78**, 465-473 (2016).
6. Edmondson, D. & von Kanel, R. Post-traumatic stress disorder and cardiovascular disease. *Lancet Psychiatry* **4**, 320-329 (2017).
7. Lowell, A., *et al.* 9/11-related PTSD among highly exposed populations: a systematic review 15 years after the attack. *Psychological medicine* **48**, 537-553 (2018).
8. Mann, F.D., *et al.* A 20-year longitudinal cohort study of post-traumatic stress disorder in World Trade Center responders. *Nature Mental Health*, 1-14 (2025).
9. Lawrence, S. & Scofield, R.H. Post traumatic stress disorder associated hypothalamic-pituitary-adrenal axis dysregulation and physical illness. *Brain Behav Immun Health* **41**, 100849 (2024).
10. Katrinli, S., Oliveira, N.C.S., Felger, J.C., Michopoulos, V. & Smith, A.K. The role of the immune system in posttraumatic stress disorder. *Transl Psychiatry* **12**, 313 (2022).
11. Picard, M. & McEwen, B.S. Psychological Stress and Mitochondria: A Systematic Review. *Psychosom Med* **80**, 141-153 (2018).
12. van der Kooij, M.A. The impact of chronic stress on energy metabolism. *Mol Cell Neurosci* **107**, 103525 (2020).
13. Geddie, H., *et al.* The impact of chronic stress on intracellular redox balance: A systems level analysis. *Physiol Rep* **11**, e15640 (2023).
14. Wolf, E.J. & Morrison, F.G. Traumatic Stress and Accelerated Cellular Aging: From Epigenetics to Cardiometabolic Disease. *Curr Psychiatry Rep* **19**, 75 (2017).
15. Wu, W. & Krijgsveld, J. Secretome Analysis: Reading Cellular Sign Language to Understand Intercellular Communication. *Mol Cell Proteomics* **23**, 100692 (2024).

16. Idle, J.R. & Gonzalez, F.J. Metabolomics. *Cell Metab* **6**, 348-351 (2007).
17. Kuan, P.-F., *et al.* Molecular linkage between post-traumatic stress disorder and cognitive impairment: a targeted proteomics study of World Trade Center responders. *Translational psychiatry* **10**, 1-15 (2020).
18. Waszczuk, M.A., *et al.* Discovery and replication of blood-based proteomic signature of PTSD in 9/11 responders. *Transl Psychiatry* **13**, 8 (2023).
19. Daskalakis, N.P., *et al.* Systems biology dissection of PTSD and MDD across brain regions, cell types, and blood. *Science* **384**, eadh3707 (2024).
20. Kuan, P.F., *et al.* Metabolomics analysis of post-traumatic stress disorder symptoms in World Trade Center responders. *Transl Psychiatry* **12**, 174 (2022).
21. Muhie, S., *et al.* Integrated analysis of proteomics, epigenomics and metabolomics data revealed divergent pathway activation patterns in the recent versus chronic post-traumatic stress disorder. *Brain Behav Immun* **113**, 303-316 (2023).
22. Halvey, P., *et al.* Variable blood processing procedures contribute to plasma proteomic variability. *Clin Proteomics* **18**, 5 (2021).
23. Kirsher, D.Y., *et al.* Current landscape of plasma proteomics from technical innovations to biological insights and biomarker discovery. *Commun Chem* **8**, 279 (2025).
24. Muhie, S., *et al.* Molecular signatures of post-traumatic stress disorder in war-zone-exposed veteran and active-duty soldiers. *Cell Rep Med* **4**, 101045 (2023).
25. Oh, H.S., *et al.* Organ aging signatures in the plasma proteome track health and disease. *Nature* **624**, 164-172 (2023).
26. Kivimaki, M., *et al.* Proteomic organ-specific ageing signatures and 20-year risk of age-related diseases: the Whitehall II observational cohort study. *Lancet Digit Health* **7**, e195-e204 (2025).
27. Dasaro, C.R., *et al.* Cohort Profile: World Trade Center Health Program General Responder Cohort. *Int J Epidemiol* **46**, e9 (2017).
28. Clouston, S., *et al.* Traumatic exposures, posttraumatic stress disorder, and cognitive functioning in World Trade Center responders. *Alzheimers Dement (N Y)* **3**, 593-602 (2017).
29. Luan, H.H., *et al.* GDF15 is an inflammation-induced central mediator of tissue tolerance. *Cell* **178**, 1231-1244. e1211 (2019).
30. Conte, M., *et al.* GDF15, an emerging key player in human aging. *Ageing Res Rev* **75**, 101569 (2022).
31. Li, X., *et al.* Lactate metabolism in human health and disease. *Signal Transduct Target Ther* **7**, 305 (2022).
32. Kobayashi, S., *et al.* Cystathionine is a novel substrate of cystine/glutamate transporter: implications for immune function. *Journal of Biological Chemistry* **290**, 8778-8788 (2015).
33. Mellon, S.H., *et al.* Metabolomic analysis of male combat veterans with post traumatic stress disorder. *PLoS One* **14**, e0213839 (2019).
34. Wang, D., *et al.* Fatty acids increase GDF15 and reduce food intake through a GFRAL signaling axis. *Diabetes* **73**, 51-56 (2024).
35. Ogłodek, E.A. Changes in the serum concentration levels of serotonin, tryptophan and cortisol among stress-resilient and stress-susceptible individuals after experiencing traumatic stress. *International Journal of Environmental Research and Public Health* **19**, 16517 (2022).

36. Sullivan, G.M., *et al.* Higher in vivo serotonin-1a binding in posttraumatic stress disorder: a PET study with [11C]WAY-100635. *Depress Anxiety* **30**, 197-206 (2013).
37. MacNamara, A., *et al.* Emotion Regulatory Brain Function and SSRI Treatment in PTSD: Neural Correlates and Predictors of Change. *Neuropsychopharmacology* **41**, 611-618 (2016).
38. Sanacora, G., Zarate, C.A., Krystal, J.H. & Manji, H.K. Targeting the glutamatergic system to develop novel, improved therapeutics for mood disorders. *Nat Rev Drug Discov* **7**, 426-437 (2008).
39. Grzesinska, A.D. The Involvement of the Endocannabinoid, Glutamatergic, and GABAergic Systems in PTSD. *Int J Mol Sci* **26**(2025).
40. Bremner, J.D., Elzinga, B., Schmahl, C. & Vermetten, E. Structural and functional plasticity of the human brain in posttraumatic stress disorder. *Prog Brain Res* **167**, 171-186 (2008).
41. Rauch, U., Feng, K. & Zhou, X.H. Neurocan: a brain chondroitin sulfate proteoglycan. *Cell Mol Life Sci* **58**, 1842-1856 (2001).
42. Li, P. & Wu, G. Roles of dietary glycine, proline, and hydroxyproline in collagen synthesis and animal growth. *Amino Acids* **50**, 29-38 (2018).
43. Yonezawa, T., *et al.* Limitrin, a novel immunoglobulin superfamily protein localized to glia limitans formed by astrocyte endfeet. *Glia* **44**, 190-204 (2003).
44. Ma, M.W., *et al.* NADPH oxidase in brain injury and neurodegenerative disorders. *Mol Neurodegener* **12**, 7 (2017).
45. O'Donovan, A., *et al.* Childhood trauma associated with short leukocyte telomere length in posttraumatic stress disorder. *Biol Psychiatry* **70**, 465-471 (2011).
46. Wolf, E.J., *et al.* Accelerated DNA Methylation Age: Associations with PTSD and Mortality. *Psychosom Med* (2017).
47. Mann, F.D., *et al.* A 20-year longitudinal cohort study of post-traumatic stress disorder in world trade Center responders. *Nature Mental Health* **3**, 789-802 (2025).
48. Weathers, F.W., Litz, B.T., Herman, D.S., Huska, J.A. & Keane, T.M. The PTSD Checklist (PCL): Reliability, validity, and diagnostic utility. in *Annual Convention of the International Society for Traumatic Stress Studies* (International Society for Traumatic Stress Studies San Antonio, 1993).
49. Kroenke, K., Spitzer, R.L. & Williams, J.B. The PHQ-9: validity of a brief depression severity measure. *J Gen Intern Med* **16**, 606-613 (2001).
50. Wisnivesky, J.P., *et al.* Persistence of multiple illnesses in World Trade Center rescue and recovery workers: a cohort study. *Lancet* **378**, 888-897 (2011).
51. An, J., *et al.* Hepatic expression of malonyl-CoA decarboxylase reverses muscle, liver and whole-animal insulin resistance. *Nat Med* **10**, 268-274 (2004).
52. Gray, N., *et al.* High-Speed Quantitative UPLC-MS Analysis of Multiple Amines in Human Plasma and Serum via Precolumn Derivatization with 6-Aminoquinolyl-N-hydroxysuccinimidyl Carbamate: Application to Acetaminophen-Induced Liver Failure. *Anal Chem* **89**, 2478-2487 (2017).
53. Bielawski, J., Szulc, Z.M., Hannun, Y.A. & Bielawska, A. Simultaneous quantitative analysis of bioactive sphingolipids by high-performance liquid chromatography-tandem mass spectrometry. *Methods* **39**, 82-91 (2006).

54. Newgard, C.B., *et al.* A branched-chain amino acid-related metabolic signature that differentiates obese and lean humans and contributes to insulin resistance. *Cell Metab* **9**, 311-326 (2009).
55. Anesi, A., *et al.* Metabolic Profiling of Human Plasma and Urine, Targeting Tryptophan, Tyrosine and Branched Chain Amino Acid Pathways. *Metabolites* **9**(2019).
56. Ehling, S. & Reddy, T.M. Investigation of the presence of beta-hydroxy-beta-methylbutyric acid and alpha-hydroxyisocaproic acid in bovine whole milk and fermented dairy products by a validated liquid chromatography-mass spectrometry method. *J Agric Food Chem* **62**, 1506-1511 (2014).
57. White, P.J., *et al.* Branched-chain amino acid restriction in Zucker-fatty rats improves muscle insulin sensitivity by enhancing efficiency of fatty acid oxidation and acyl-glycine export. *Mol Metab* **5**, 538-551 (2016).
58. Gene Ontology, C. The Gene Ontology (GO) project in 2006. *Nucleic Acids Res* **34**, D322-326 (2006).
59. Ogata, H., *et al.* KEGG: Kyoto Encyclopedia of Genes and Genomes. *Nucleic Acids Res* **27**, 29-34 (1999).
60. Hyvarinen, A. Fast and robust fixed-point algorithms for independent component analysis. *IEEE Trans Neural Netw* **10**, 626-634 (1999).

Acknowledgments

We gratefully acknowledge the support of the first responders and rescue/recovery workers through their participation in this study. We also thank the staff of the Stony Brook World Trade Center Health Program and the World Trade Center Health Program Data Monitoring Center for ongoing support. The findings and conclusions presented in this article are those of the authors and do not represent the official position of NIOSH, the CDC, NIH or the U.S. Public Health Service. During manuscript preparation, the authors used a generative AI tool for language refinement and consultation of general background information during the literature review. All scientific interpretations, data analyses, and conclusions were developed solely by the research team, who take full responsibility for the content.

Funding Statement

The current study was supported in part by CDC/NIOSH, NIH/NIA and NIH/NIDDK awards: CDC-75D30122c15522 (PI: Benjamin Luft), U01 OH012466 (PI: Pei Fen Kuan), R21 AG081480 (PI: Pei Fen Kuan), U01 OH012257 (MPI: Pei Fen Kuan, Sean Clouston), P30 DK124723 (PI: Christopher Newgard) and the SUNY Research Foundation.

Author Contributions Statement

The authors confirm contribution to the paper as follows: Study conception, design, and funding acquisition: P.K., B.J.L. Plasma sample retrieval and coordination of the proteomic and metabolomic assays: X.Y. Metabolomics assay generation: O.I., M.M. Data analysis, primary interpretation of results, and drafting of the original manuscript: P.K. Proteomic and metabolomic interpretation: C.B.N. Critical revision of the manuscript for important intellectual content: F.D.M.,

X.Y., R.K., S.C., O.I., M.M., C.B.N., B.J.L. All authors reviewed the results and approved the final manuscript.

Competing Interest Statement

The authors declare no competing interests.

Tables

Table 1. Clinical characteristics of the study sample. P-values were derived using two-sided t-tests for continuous variables (age, BMI, and PHQ score) and two-sided chi-squared tests for categorical variables (gender, race, smoking status, WTC exposure, NSAID use, SSRI use, statin use, and medical comorbidity). Missing categories were excluded from chi-square tests for smoking status and WTC exposure. Medical comorbidity was defined as the presence of COPD, cardiac disease, diabetes, hypertension, or stroke. Exact *p*-values are reported where possible.

Variable	PTSD *n* = 232	Trauma-exposed control *n* = 161	P-value
Age			
Mean (SD)	56.6 (7.8)	53.8 (7.2)	2.0×10^{-4}
Gender N (%)			
Male	208 (90)	148 (92)	0.560
Female	24 (10)	13 (8)	
Race N (%)			
White	203 (88)	137 (85)	0.591
Other	29 (12)	24 (15)	
BMI			
Mean (SD)	31.7 (5.9)	29.8 (4.6)	3.7×10^{-4}
PHQ score			
Mean (SD)	13.3 (6.2)	0.47 (1.0)	$< 1 \times 10^{-15}$
Smoking N (%)			
Current	26 (11)	20 (12)	0.107
Former	77 (33)	38 (24)	
Never	127 (55)	103 (64)	
Missing	2 (1)	0 (0)	
WTC exposure N (%)			
Low	21 (9)	30 (19)	0.0017
Intermediate	145 (63)	100 (62)	
High	40 (17)	21 (13)	
Very high	14 (6)	1 (1)	
Missing	12 (5)	9 (5)	
NSAID use N (%)			
Yes	48 (21)	20 (12)	0.046
No	184 (79)	141 (88)	
SSRI use N (%)			
Yes	68 (29)	0 (0)	1.2×10^{-13}
No	164 (71)	161 (100)	
Statin use N (%)			
Yes	67 (29)	38 (24)	0.295
No	165 (71)	123 (76)	
Medical comorbidity (any) N (%)			
Yes	140 (60)	53 (33)	1.6×10^{-7}
No	92 (40)	108 (67)	

Table 2. Subset of differentially expressed (DE) aptamer-based protein analytes identified in the present study that were replicated in other studies, namely WTC Study 1 (Kuan et al. [17]), PSYCHENCODE2-UKBB [19], and Muhie et al. [24]. For WTC Study 1 (Kuan et al. [17]) and PSYCHENCODE2-UKBB [19], we report the effect size (ES) direction and whether the protein was significant at FDR < 0.05 in the original study (***).

AptName	Target	Gene Symbol	ES	WTC Study1 Kuan	PSYENCODE2 UKBB	Military
seq.4498.62	NCAM-120	NCAM1	Down		Down ***	Yes
seq.20161.41	NCAM1	NCAM1	Down		Down ***	Yes
seq.15573.110	CSPG3	NCAN	Down	Down ***		
seq.27221.34	Myostatin-Propeptide	MSTN	Down	Down	Down ***	
seq.4374.45	MIC-1	GDF15	Up		Up ***	
seq.34255.32	ATS8	ADAMTS8	Down		Down ***	
seq.16818.200	CDCP1	CDCP1	Up		Up ***	
seq.2677.1	ERBB1	EGFR	Down			Yes
seq.6556.5	ENPP5	ENPP5	Down		Down ***	
seq.4559.64	KYNU	KYNU	Up	Up	Up ***	
seq.5635.66	TREM2	TREM2	Up		Up ***	
seq.30695.4	PON3	PON3	Down		Down ***	
seq.3461.58	PGCB	BCAN	Down	Down ***	Down ***	
seq.2201.17	Endostatin	COL18A1	Up		Up ***	
seq.31918.65	EST2	CES2	Up		Up ***	
seq.3216.2	PIGR	PIGR	Up	Down	Up ***	
seq.5483.1	RGMA	RGMA	Down	Down	Down ***	
seq.7182.1	carboxylesterase, liver	CES1	Up		Up ***	
seq.3339.33	TSP2	THBS2	Up	Up		
seq.11196.31	Collagen alpha-3(VI):BPTI/Kunitz inhibitor	COL6A3	Up		Up ***	
seq.5307.12	Coagulation Factor IXab	F9	Up		Up ***	
seq.9282.12	CRIS2	CRISP2	Down		Down ***	
seq.2974.61	contactin-1	CNTN1	Down		Down ***	Yes
seq.11851.21	TREM2	TREM2	Up		Up ***	
seq.10970.3	NAR3	ART3	Down		Down ***	
seq.16300.4	TREM2	TREM2	Up		Up ***	
seq.5353.89	IL-1Ra	IL1RN	Up	Up	Up ***	
seq.29534.9	FGF21	FGF21	Up	Up	Up ***	
seq.4568.17	SLIK5	SLITRK5	Down			Yes
seq.20590.13	NPY	NPY	Down		Up ***	

seq.5452.71	ASGR1	ASGR1	Up	Up	Up ***	
seq.19241.31	RBP-III	RBP5	Up		Up ***	
seq.15386.7	FABPA	FABP4	Up		Up ***	
seq.16307.22	UNC5H4	UNC5D	Down			Yes
seq.15487.164	carboxylesterase, liver	CES1	Up		Up ***	
seq.3446.7	IL-18 Ra	IL18R1	Up		Up ***	
seq.9377.25	SCF	KITLG	Down	Down		

Table 3. Gene Ontology (GO) categories significantly enriched at FDR < 0.1.

Ontology	ID	Description	Major theme
CC	GO:0030312	external encapsulating structure	Structural/Extracellular Matrix
CC	GO:0031012	extracellular matrix	Structural/Extracellular Matrix
CC	GO:0062023	collagen-containing extracellular matrix	Structural/Extracellular Matrix
BP	GO:0099560	synaptic membrane adhesion	Structural/Extracellular Matrix
BP	GO:0097106	postsynaptic density organization	Structural/Extracellular Matrix
BP	GO:0031102	neuron projection regeneration	Neuronal/Nervous System
BP	GO:0031103	axon regeneration	Neuronal/Nervous System
BP	GO:0048678	response to axon injury	Neuronal/Nervous System
BP	GO:0048679	regulation of axon regeneration	Neuronal/Nervous System
BP	GO:0070570	regulation of neuron projection regeneration	Neuronal/Nervous System
BP	GO:0070571	negative regulation of neuron projection regeneration	Neuronal/Nervous System
BP	GO:0061564	axon development	Neuronal/Nervous System
BP	GO:0051960	regulation of nervous system development	Neuronal/Nervous System
BP	GO:0050767	regulation of neurogenesis	Neuronal/Nervous System
BP	GO:0010001	glial cell differentiation	Neuronal/Nervous System
BP	GO:0042063	gliogenesis	Neuronal/Nervous System
BP	GO:0021782	glial cell development	Neuronal/Nervous System
BP	GO:0031099	regeneration	Developmental/Growth Regulation
BP	GO:0042554	superoxide anion generation	Immune/Oxidative Stress/Inflammation
BP	GO:0009410	response to xenobiotic stimulus	Immune/Oxidative Stress/Inflammation
BP	GO:0071466	cellular response to xenobiotic stimulus	Immune/Oxidative Stress/Inflammation
BP	GO:0009749	response to glucose	Metabolic/Nutrient Response
BP	GO:0009746	response to hexose	Metabolic/Nutrient Response
BP	GO:0034284	response to monosaccharide	Metabolic/Nutrient Response
CC	GO:0005788	endoplasmic reticulum lumen	Cellular Components (Intracellular)

Table 4. Spearman rank correlations between predicted organ age measures and chronological age.

Organ	r_s
Conventional	0.843
Organismal	0.826
CognitionOrganismal	0.721
Immune	0.561
Liver	0.46
Brain	0.401
Pancreas	0.395
Intestine	0.388
Muscle	0.381
CognitionLiver	0.367
CognitionIntestine	0.365
CognitionHeart	0.355
Heart	0.355
CognitionPancreas	0.353
CognitionBrain	0.336
Artery	0.313
CognitionImmune	0.311
CognitionMuscle	0.31
CognitionArtery	0.309
Lung	0.302
Kidney	0.298
Adipose	0.283
CognitionAdipose	0.27
CognitionKidney	0.268
CognitionLung	0.222

Figure Legends/Captions

Figure 1. (A) Volcano plot of differential protein expression. **(B)** Volcano plot of differential metabolite expression. **(C)** Heatmap of the 121 aptamer-based protein analytes significantly associated with PTSD at FDR < 0.05. **(D)** Heatmap of the 7 metabolites significantly associated with PTSD at FDR < 0.05. Differential expression analyses were performed using two-sided linear regression models with HC3 robust standard errors, adjusting for age, gender, and race. Multiple testing correction was performed using the Benjamini-Hochberg false discovery rate procedure. Source data are provided as a Source Data file.

Figure 2. (A) Heatmap summarizing significant protein-metabolite correlations (FDR < 0.05, denoted by *), identified from differential expression analysis. Rows represent aptamer-based protein analytes and columns represent metabolites. **(B-D)** Representative examples of protein-metabolite pairs showing nominal interaction effects ($p < 0.01$) by PTSD status. Scatterplots illustrate differential slopes between participants with PTSD and trauma-exposed controls: **(B)** NCAN versus cystathionine. **(C)** NOX4 versus cystathionine. **(D)** MXRA8 versus hydroxylysine. Protein-metabolite correlations in panel A were evaluated using two-sided Spearman rank correlation tests with Benjamini-Hochberg false discovery rate correction applied within metabolite. Interaction effects in panels B-D were evaluated using two-sided linear regression models including protein analyte × PTSD interaction terms, adjusting for age, gender, and race. Statistical inference was based on HC3 robust standard errors. Shaded bands represent 95% confidence intervals around fitted linear regression lines. Source data are provided as a Source Data file.

Figure 3. Associations between chronological age and predicted proteomic age measures, and comparison of age acceleration by PTSD status. Scatterplots comparing chronological age with predicted age are shown in the top row, and boxplots comparing organ aging between individuals with PTSD and trauma-exposed controls are shown in the bottom row for organ systems significantly associated with PTSD. **(A)** Pancreas. **(B)** CognitionLung. **(C)** Organismal. **(D)** CognitionOrganismal. **(E)** Conventional. Each point represents an independent participant sample from the WTC responder cohort ($n = 391$ biologically independent plasma samples with SomaScan data; PTSD = 231, trauma-exposed controls = 160). No technical replicates were used in the statistical analyses. In the boxplots, the center line represents the median, box bounds represent the 25th and 75th percentiles, and whiskers extend to the smallest and largest values within 1.5 × IQR from the hinges. Individual participant values are overlaid as jittered points. Source data are provided as a Source Data file.

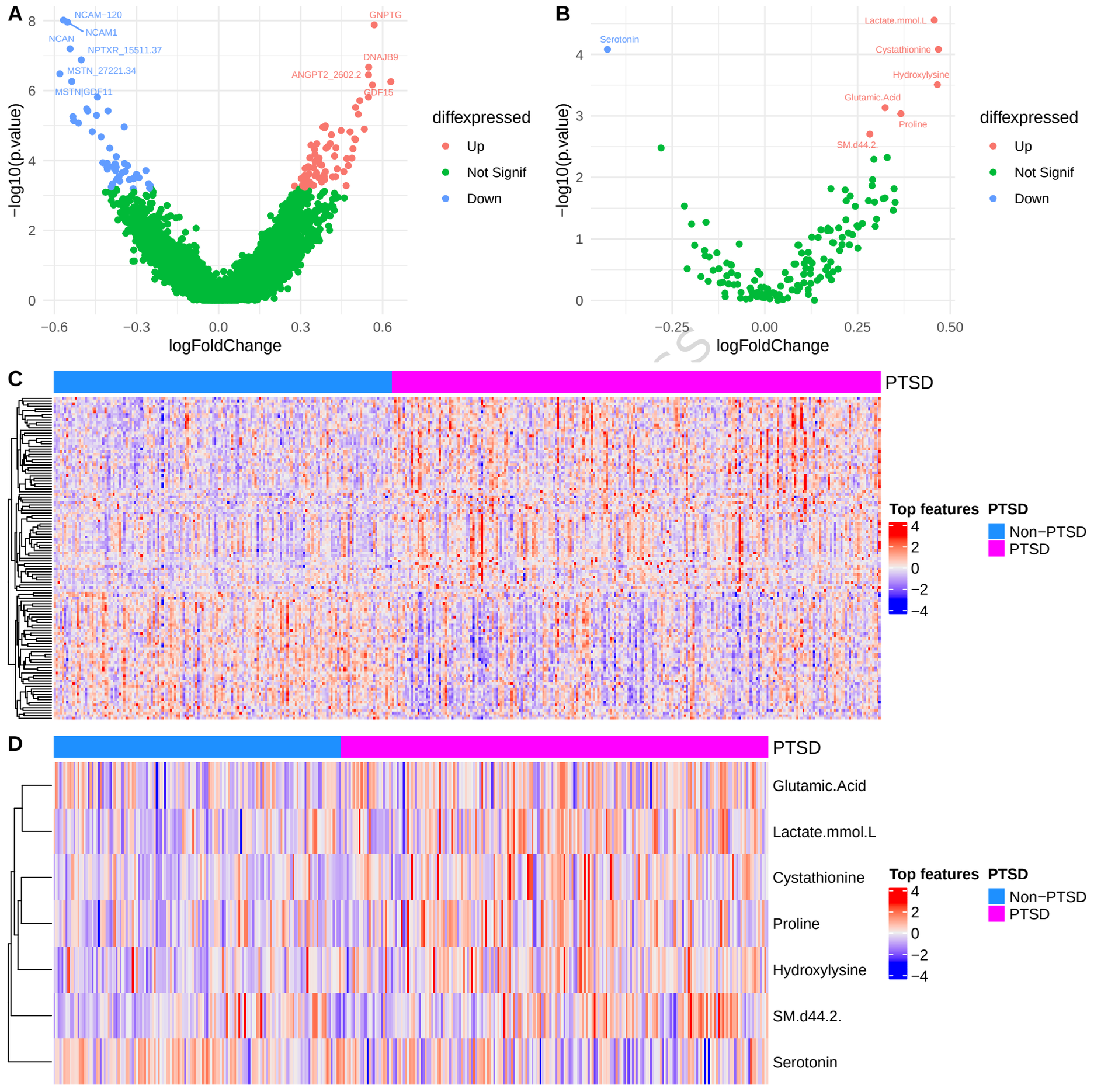
A
NCAM−120
NCAM1
NCAN
NPTXR_15511.37
MSTN_27221.34
MSTN|GDF11
GNPTG
DNAJB9
ANGPT2_2602.2
GDF15
−log10(p.value)
logFoldChange
diffexpressed
Up
Not Signif
Down
B
Serotonin
Lactate.mmol.L
Cystathionine
Hydroxylysine
Glutamic.Acid
Proline
SM.d44.2.
−log10(p.value)
logFoldChange
diffexpressed
Up
Not Signif
Down
C
PTSD
Top features
PTSD
Non−PTSD
PTSD
D
PTSD
Glutamic.Acid
Lactate.mmol.L
Cystathionine
Proline
Hydroxylysine
SM.d44.2.
Serotonin
Top features
PTSD
Non−PTSD
PTSD

A

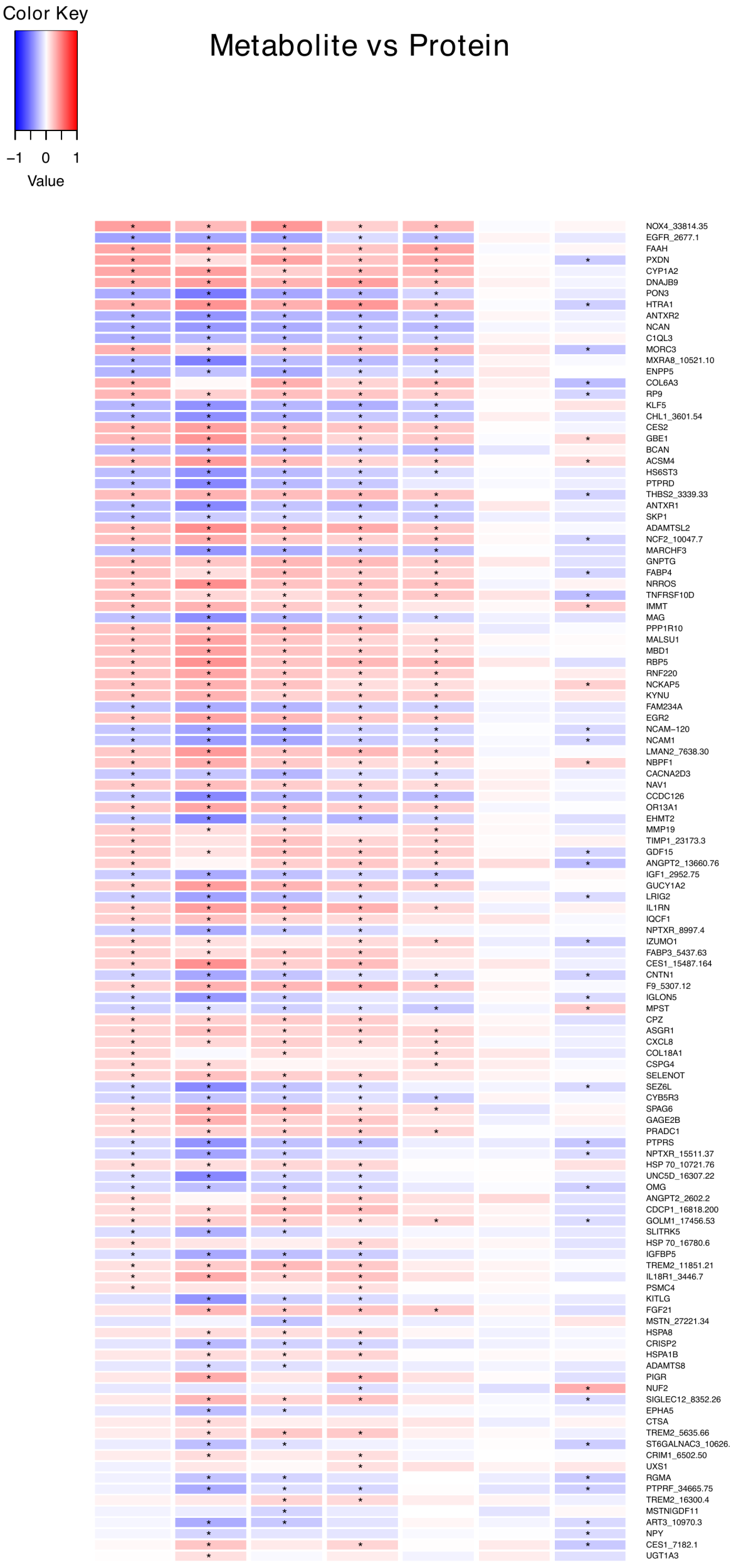
Color Key
−1 0 1
Value
Metabolite vs Protein
NOX4_33814.35
EGFR_2677.1
FAAH
PXDN
CYP1A2
DNAJB9
PON3
HTRA1
ANTXR2
NCAN
C1QL3
MORC3
MXRA8_10521.10
ENPP5
COL6A3
RP9
KLF5
CHL1_3601.54
CES2
GBE1
BCAN
ACSM4
HS6ST3
PTPRD
THBS2_3339.33
ANTXR1
SKP1
ADAMTSL2
NCF2_10047.7
MARCHF3
GNPTG
FABP4
NRROS
TNFRSF10D
IMMT
MAG
PPP1R10
MALSU1
MBD1
RBP5
RNF220
NCKAP5
KYNU
FAM234A
EGR2
NCAM−120
NCAM1
LMAN2_7638.30
NBPF1
CACNA2D3
NAV1
CCDC126
OR13A1
EHMT2
MMP19
TIMP1_23173.3
GDF15
ANGPT2_13660.76
IGF1_2952.75
GUCY1A2
LRIG2
IL1RN
IQCF1
NPTXR_8997.4
IZUMO1
FABP3_5437.63
CES1_15487.164
CNTN1
F9_5307.12
IGLON5
MPST
CPZ
ASGR1
CXCL8
COL18A1
CSPG4
SELENOT
SEZ6L
CYB5R3
SPAG6
GAGE2B
PRADC1
PTPRS
NPTXR_15511.37
HSP 70_10721.76
UNC5D_16307.22
OMG
ANGPT2_2602.2
CDCP1_16818.200
GOLM1_17456.53
SLITRK5
HSP 70_16780.6
IGFBP5
TREM2_11851.21
IL18R1_3446.7
PSMC4
KITLG
FGF21
MSTN_27221.34
HSPA8
CRISP2
HSPA1B
ADAMTS8
PIGR
NUF2
SIGLEC12_8352.26
EPHA5
CTSA
TREM2_5635.66
ST6GALNAC3_10626.116
CRIM1_6502.50
UXS1
RGMA
PTPRF_34665.75
TREM2_16300.4
MSTNIGDF11
ART3_10970.3
NPY
CES1_7182.1
UGT1A3
Cystathionine
Glutamic.Acid
Hydroxylysine
Lactate.mmol.L
Proline
SM.d44.2.
Serotonin

B

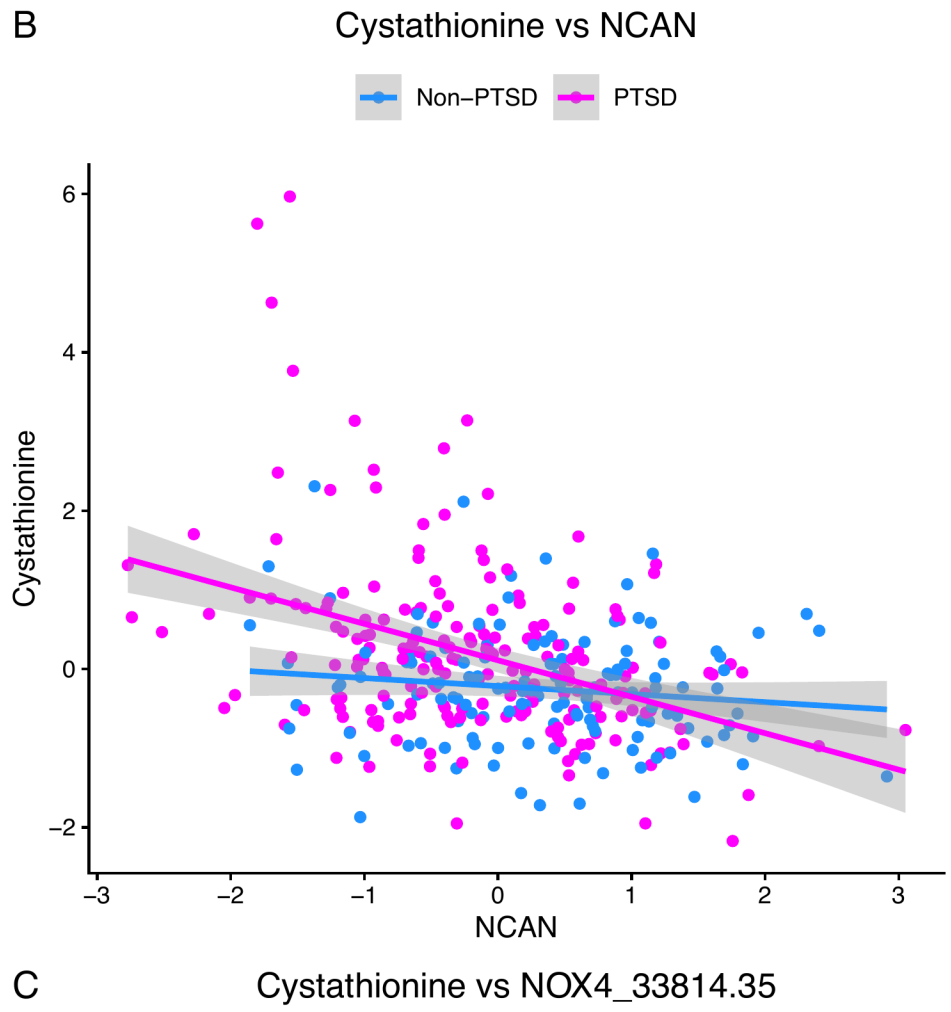
Cystathionine vs NCAN
Non−PTSD
PTSD
Cystathionine
NCAN

C

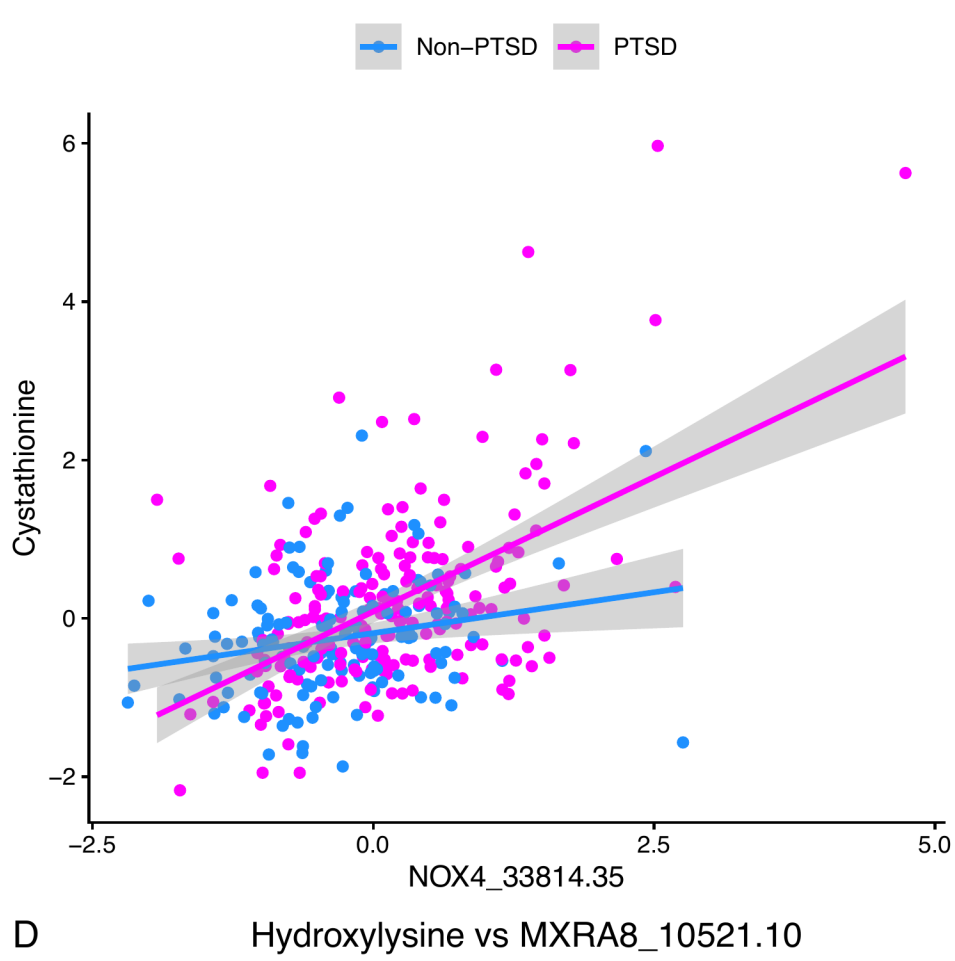
Cystathionine vs NOX4_33814.35
Non−PTSD
PTSD
Cystathionine
NOX4_33814.35

D

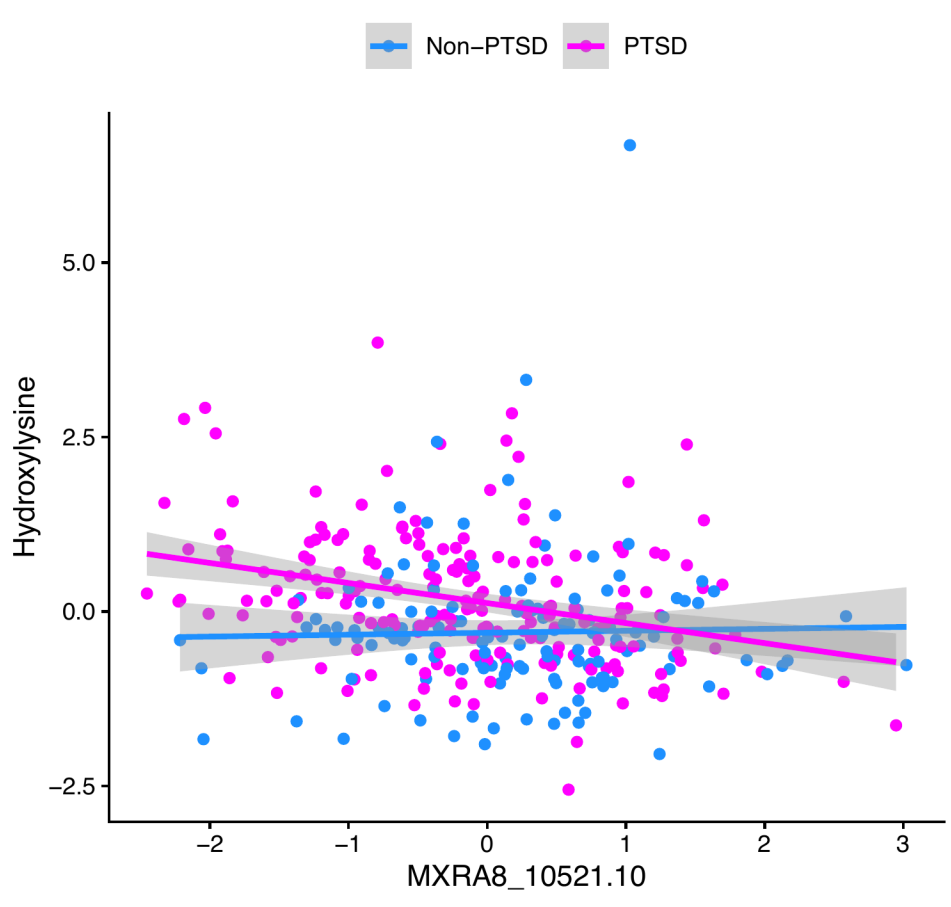
Hydroxylysine vs MXRA8_10521.10
Non−PTSD
PTSD
Hydroxylysine
MXRA8_10521.10

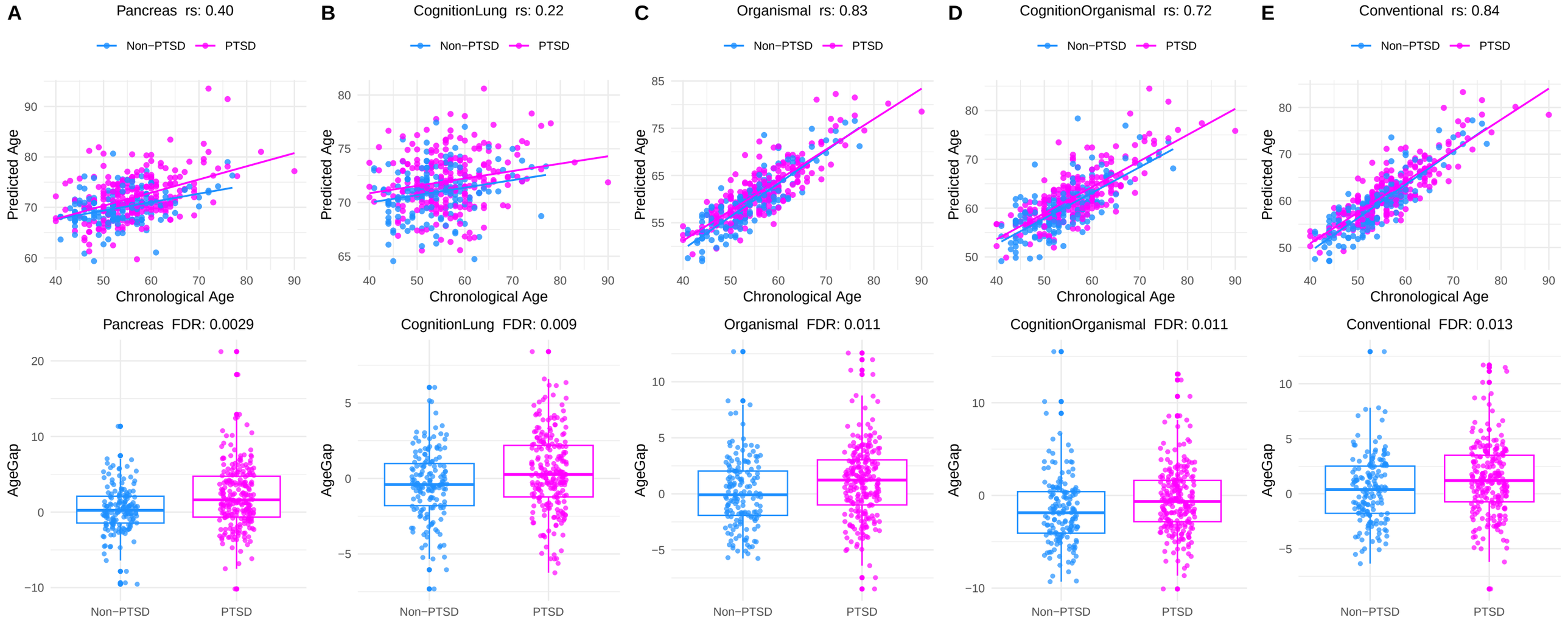
A
Pancreas rs: 0.40
Non−PTSD
PTSD
Predicted Age
Chronological Age
Pancreas FDR: 0.0029
AgeGap
Non−PTSD
PTSD
B
CognitionLung rs: 0.22
Non−PTSD
PTSD
Predicted Age
Chronological Age
CognitionLung FDR: 0.009
AgeGap
Non−PTSD
PTSD
C
Organismal rs: 0.83
Non−PTSD
PTSD
Predicted Age
Chronological Age
Organismal FDR: 0.011
AgeGap
Non−PTSD
PTSD
D
CognitionOrganismal rs: 0.72
Non−PTSD
PTSD
Predicted Age
Chronological Age
CognitionOrganismal FDR: 0.011
AgeGap
Non−PTSD
PTSD
E
Conventional rs: 0.84
Non−PTSD
PTSD
Predicted Age
Chronological Age
Conventional FDR: 0.013
AgeGap
Non−PTSD
PTSD